Original Paper

Control of different occurrence types of organic matter on hydrocarbon generation in mudstones

Peng-Yan Du [a], Jin-Gong Cai [a, *], Qing Liu [b], Xue-Jun Zhang [b], Juan Wang [b]

[a] State Key Laboratory of Marine Geology, Tongji University, Shanghai, 200092, China
[b] Exploration and Development Research Institute of Shengli Oilfield Company, SINOPEC, Dongying, Shandong 257001, China

ABSTRACT

Organic matter (OM) is preserved as different occurrences in mudstones, which can affect the hydrocarbon generation process. However, little research has focused on hydrocarbon generation as a function of different occurrences of OM. This study collected a suite of mudstones in the Dongying Sag, Bohai Bay Basin, and conducted Rock-Eval VI pyrolysis after Soxhlet extraction and $Na_2S_2O_8$ oxidation, aiming to quantify the OM with different occurrences and figure out the contributions of each occurrence of OM to the hydrocarbon generation. There are three types of occurrences of OM: soluble organic matter (SOM), mineral-bound organic matter (MOM), and particulate organic matter (POM). MOM is the most abundant among the three occurrence types of OM. SOM and MOM are the main hydrocarbon precursors, and their hydrocarbon contributions alternate with different kerogen types and layers. Additionally, MOM-contributed hydrocarbons are numerous at shallow depths; SOM-contributed hydrocarbons mainly occur at deep depths; and POM-contributed hydrocarbons change little with depth. These results demonstrate that MOM should be the main hydrocarbon precursor in shallow formations and that SOM is the main hydrocarbon contributor at deep depths.

1. Introduction

Different types of occurrences of OM in source rocks have received much attention in the areas of petroleum generation and the global carbon cycle (Berthonneau et al., 2016; Cai et al., 2007; Jarvie et al., 2007; Kennedy and Wagner, 2011; Rahman et al., 2017). Learning the characteristics of different types of occurrences of OM would be significantly useful for further understanding hydrocarbon generation mechanisms in source rocks.

Various studies have focused on OM classification in source rocks according to the OM occurrence (Kennedy et al., 2002; Zhu et al., 2016), and the physicochemical interactions between OM and clay minerals (Cai et al., 2020; Keil and Maye, 2014; Lützow et al., 2006; Zhu et al., 2020). Soluble and insoluble OM (Durand, 1980; Tissot and Welte, 1984), OM combined with minerals and not combined with minerals (Keil and Mayer, 2014), and structured and amorphous OM (Sebag et al., 2006; Tyson, 1995) demonstrate the diversity of OM. The OM combined with minerals have various

bonding mechanisms with mineral surfaces, such as ligand exchange (Kaiser et al., 2007; Kleber et al., 2007), ion exchange (Mikutta et al., 2007, 2009), cation bridging (Li et al., 2015; Lützow et al., 2006), etc. Soluble OM is generally in a free state or physically adsorbed in source rocks (Tissot and Welte, 1984). As the OM with different occurrences have different structures and hydrocarbon generation mechanisms, they may contribute different volumes of hydrocarbons to source rocks (Kennedy et al., 2014; Rahman et al., 2018; Tissot and Welte, 1984; Yuan et al., 2013). However, there are currently few studies on the specific differences in hydrocarbon contributions of the OM with different occurrences.

Previous studies have employed many methods to separate different occurrences of OM. Soxhlet extraction (Tissot and Welte, 1984), density fractionation (Arnarson and Keil, 2001), and size fractionation (Carter et al., 2003) are always used to separate soluble OM. The OM combined with minerals can be removed by oxidizing agents such as H_2O_2, NaClO, and $Na_2S_2O_8$ (Eusterhues et al., 2003; Kiem et al., 2002; Meier and Menegatti, 1997; Mikutta et al., 2005), among which $Na_2S_2O_8$ is considered to be more efficient (Helfrich et al., 2007; Lützow et al., 2007). However, quantifying OM with different types of occurrences in source rocks

* Corresponding author.
  E-mail address: jgcai@tongji.edu.cn (J.-G. Cai).

is still a difficult problem.

This work collected a suite of mudstones in the Dongying Sag in the depth range of 1850−5000 m. Soxhlet extraction and $Na_2S_2O_8$ oxidation were used to sequentially remove OM with different occurrences from the mudstones, respectively. Subsequently, the quantification of OM with different occurrences was realized by conducting Rock-Eval VI pyrolysis on raw, Soxhlet extracted, and $Na_2S_2O_8$ oxidized mudstones. Correspondingly, the hydrocarbon generation potential and behavior of OM with different occurrences were investigated in the whole depth profile.

2. Materials and methods

2.1. Materials

The samples in this work are from the Dongying Sag in the Jiyang Depression in the Bohai Bay Basin, which is located in the northern part of Shandong Province, China (Fig. 1a). The Dongying Sag is an important petroliferous sag with an exploration area of approximately 5850 km^2 (Du et al., 2019; Zhang et al., 2009). The tectonic evolution of Dongying Sag has gone through four stages: the pre-rift stage, the rift stage, the fault stage, and the depression stage (Feng et al., 2013). The sag is bounded by the Chenjiazhuang Uplift onto the north, the Qingtuozi and Guangrao Uplift on to the east, the Luxi Uplift onto the south, and the Qingcheng-Linjia-Binxian Uplift onto the west (Fig. 1a). The Cenozoic strata in the Dongying Sag includes Paleogene, Neogene and Quaternary lacustrine deposits. The Paleogene has been divided into Kongdian (Ek), Shahejie (Es), and Dongying (Ed) Formations from bottom upward (Bai et al., 2018; Zeng et al., 2018) (Fig. 1b). Es has been further divided into four members called the Fourth Member (Es$_4$), the Third Member (Es$_3$), the Second Member (Es$_2$), and the First Member (Es$_1$) from bottom upward (Bai et al., 2018). Es$_3$ and Es$_4$ are the main source rock layers in the Dongying Sag, which developed a large set of lacustrine shales deposits (Zou et al., 2018). From Es$_4$ up to Es$_3$, the water in the lake basin of the Dongying Sag experienced a process of changing from shallow to deep, and then to shallow, and the salinity of the sedimentary water body gradually decreased. Es$_4$ has been divided into two sub-members, the lower sub-member of Es$_4$ (Es$_4^{Lower}$) and the upper sub-member of Es$_4$ (Es$_4^{Upper}$), and Es$_3$ has been divided into three sub-members, the lower sub-member of Es$_3$ (Es$_3^{Lower}$), the middle sub-member of Es$_3$ (Es$_3^{Middle}$), and the upper sub-member of Es$_3$ (Es$_3^{Upper}$) (Fig. 1b).

A total of 29 mudstone samples from depths of 1850−5000 m were collected from the Shahejie Formation within 12 wells. The samples are mostly dark-gray mudstones, and three samples are from the following members: Es$_1$, Es$_2$ and Es$_3^{Upper}$. Six samples are from the Es$_3^{Middle}$ member, seven samples are from the Es$_3^{Lower}$ member, eleven samples are from the Es$_4^{Upper}$ member and two samples are from the Es$_4^{Lower}$ member. Information for these samples is shown in Table S1 in the Supplementary Data.

2.2. Methods

The samples were crushed into powder, screened to a 100-mesh (< 0.15 mm), and then dried for 24 h at 60 °C. The dried samples were stored in a desiccator for further experiments.

2.2.1. Soxhlet extraction

First, approximately 10 g of sample powder was wrapped with filter paper and weighed, and then refluxed with a mixture of CH_2Cl_2:CH_3OH at a ratio of 9:1 (vol:vol) in a Soxhlet extractor to
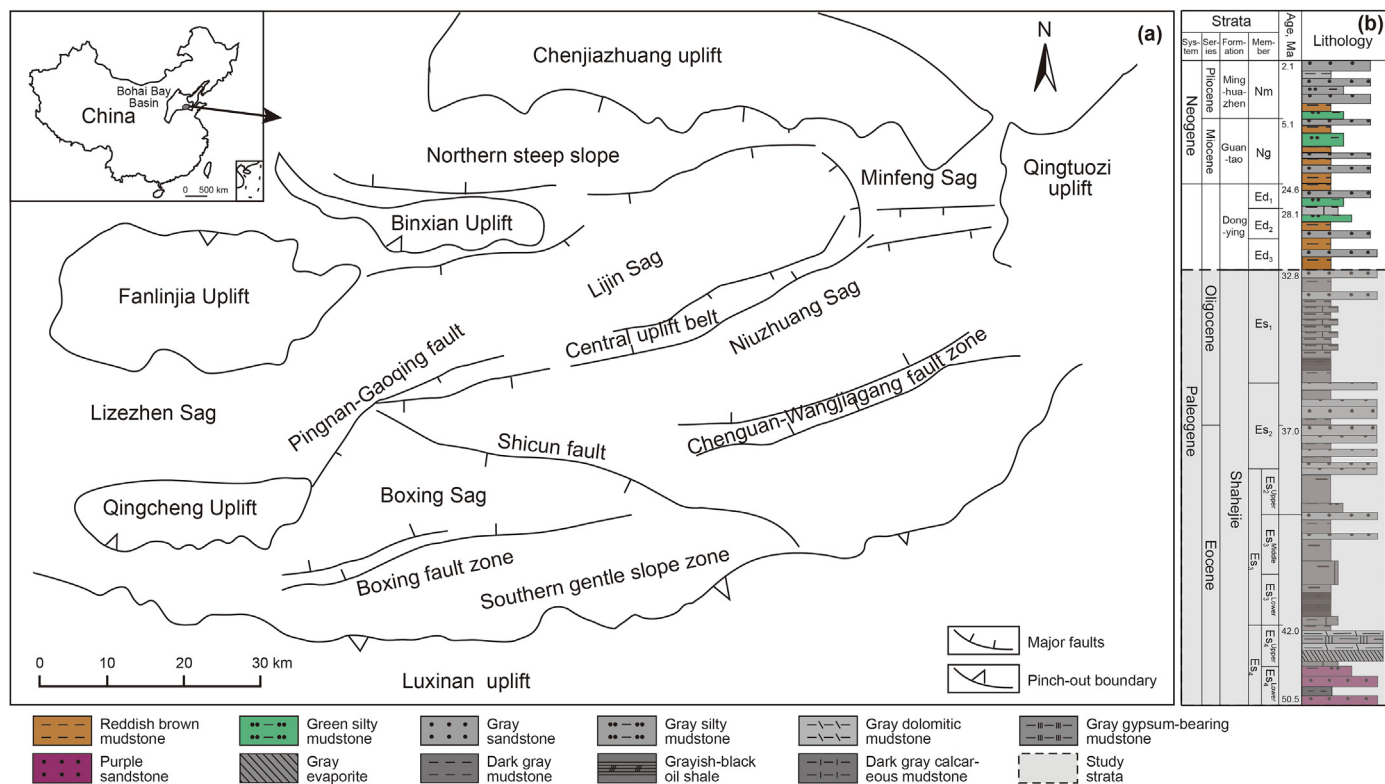

Fig. 1. Location map and development of strata in the Dongying Sag (modified by Zeng et al. (2018)). (**a**) Study area and structural units of the Dongying Sag in the Bohai Bay Basin, China (the gray dot denotes the Dongying Sag). (**b**) Development of Paleogene deposits in the Dongying Sag (the gray shading indicates the research strata).

remove the soluble OM (Cai et al., 2021). Then, the extraction was conducted at 48 °C for 72 h. Last, the extraction residues were dried at 60 °C for 24 h and weighed. The analytical balance was a Mettler Toledo ME104, its resolution was 0.0001 g, and the maximum permission error (MPE) was 0.0002 g.

2.2.2. $Na_2S_2O_8$ oxidation

The Soxhlet extraction residues were then subjected to $Na_2S_2O_8$ oxidation, which could oxidize the OM combined with minerals without damage to the mineral structure (Kiem et al., 2002; Menegatti et al., 1999). The oxidizing solvent was a mixture of $Na_2S_2O_8$:$NaHCO_3$ at a mass ratio of 1:1.1 (g:g). The mass ratio of the sample to $Na_2S_2O_8$ is approximately 1:40 (g:g) (Meier and Menegatti, 1997; Mikutta et al., 2005). First, approximately 2 g of Soxhlet extraction residue was weighed and dispersed in oxidizing solvent diluted with deionized water to a total volume of 1000 mL with a pH of 7–8.5 (Cai et al., 2021). Then, the oxidation treatment was performed in a water bath at 80 °C for 48 h. Next, the oxidation residues were washed with deionized water several times to remove sulfate ions. Last, the washed residues were dried at 60 °C for 48 h and weighed.

2.2.3. Rock-Eval VI pyrolysis

Rock-Eval VI pyrolysis (Vinci Technologies, France) experiments were conducted in the Experimental Research Center of the Wuxi Petroleum Geology Institute, China Petroleum & Chemical Corporation (SINOPEC). The sample was heated at 300 °C in helium flow for 2.5 min, then heated from 300 °C to 650 °C with a heating rate of 25 °C/min, and the hydrocarbon released was detected by a hydrogen flame ionization detector. CO_2 released during pyrolysis was detected by a thermal conductivity detector. Pyrolysis was conducted on all of the raw, extracted and oxidized samples to obtain the pyrolysis parameters of total organic carbon (TOC) content, free hydrocarbons (S1), pyrolysis hydrocarbons (S2), the hydrogen index (HI = S2/TOC), and the temperature of the maximum S2 peak (T_{max}) (Behar et al., 2001; Carrie et al., 2012).

3. Results

The TOC contents of the raw samples first increased and then decreased with depth (Fig. 2a). The TOC contents of approximately 45% of the samples were in the range of 2%–4%, approximately 14% of the samples had TOC contents higher than 4%, 31% of the samples had TOC contents in the range of 1%–2%, and only approximately 10% of the samples had TOC contents less than 1% (Fig. 2b). The S1 and S2 of the raw samples all increased in shallow formations and then decreased with depth; the S1 values were 0–8 mg/g, and the S2 values were 0–110 mg/g (Fig. 2c and d). The kerogen types in the raw samples in each layer were mainly types I and II (Fig. 2e).

The TOC contents of the extracted samples had a similar evolutionary trend to that of the raw samples (Fig. 2a), but approximately 53% of the TOC contents of the extracted samples were in the 1%–2% range, approximately 27% were in the 2%–4% range, 10% were less than 1% and 10% were larger than 4% (Fig. 2b). S1 values of the extracted samples were mostly less than 0.1 mg/g (Fig. 2c). S2 values of the extracted samples had a similar trend to the S2 values of the raw samples, and the TOC values of the extracted samples were slightly lower (Fig. 2d). The kerogen types of the extracted samples were mainly I and II, while some samples in Es_4^{Upper} change to type III (Fig. 2f).

After the subsequent $Na_2S_2O_8$ oxidation, the TOC contents of the oxidized samples generally changed little with depth (Fig. 2a), and the TOC values of approximately 76% oxidized samples were less than 1%, approximately 14% were in the 1%–2% range, 7% were in the 2%–4% range, and only 3% were higher than 4% (Fig. 2b). S1 values of the oxidized samples were nearly 0 mg/g (Fig. 2c), and S2 values were less than 2 mg/g (Fig. 2d). The kerogen types of the oxidized samples mostly changed to types II and III (Fig. 2g).

4. Discussion

4.1. Definition of OM with different occurrences

The sequential treatment results show that OM in mudstones is mostly removed by Soxhlet extraction and $Na_2S_2O_8$ oxidation (Fig. 2a and b). As Soxhlet extraction is a physical action that has no influence on the structure of organic matters, the organic matter that is dissolved in this process is physically adsorbed in mudstones and is defined as soluble organic matter (SOM) (Tissot and Welte, 1984). $Na_2S_2O_8$ oxidation is a chemical reaction that can yield SO_4^- radicals that react with OM (Mikutta et al., 2005; Zhu et al., 2016). As $Na_2S_2O_8$ oxidation was treated sequentially after Soxhlet extraction, the OM removed in this process is bonding to the clay mineral interlayer or mineral surface (Helfrich et al., 2007; Lützow et al., 2007). This kind of OM is mainly an amorphous component (Cai et al., 2007, 2020; Zhu et al., 2020) and is defined as mineral-bound organic matter (MOM) in this paper (Fig. 3). Thus, SOM and MOM could be progressively removed by the two sequential treatments. There is also a small amount of OM in the $Na_2S_2O_8$ oxidized sample (Fig. 2a). As this kind of OM is mainly clumpy flocs or macromolecule polymers that can barely be physically or chemically removed (Cambardella and Elliott, 1992; Keil and Mayer, 2014; Lopez-Sangil and Rovira, 2013), it is defined as particulate organic matter (POM) in this work (Fig. 3).

4.2. Quantification of OM with different occurrences

The contents of SOM, MOM and POM can be represented by the TOC difference between the raw, extracted and oxidized samples. The hydrocarbons generated from SOM, MOM and POM can be calculated based on S1 and S2 of the raw, extracted and oxidized samples. As the denominators of TOC, S1 and S2 of the raw, extracted and oxidized samples are different, these parameters need to be calculated with the same denominator, and then the abundances and hydrocarbon parameters of SOM, MOM and POM can be calculated.

The quantification process mainly involves two steps: first, the sample weights of the raw, extracted and oxidized samples are used to calculate the conversion factors (f_e, f_o), which can convert TOC, S1 and S2 of the raw, extracted, and oxidized samples to have the same denominator; second, the difference between the converted TOC, S1 and S2 of the raw, extracted, and oxidized samples is calculated to obtain the abundances and hydrocarbon contents of SOM and MOM. The calculation equations for the two steps are shown by Eq. (1)–Eq. (5) in Fig. 4.

The sum of S1 and S2 can be used to represent the total hydrocarbons (TS) generated from each OM with different occurrences (Eq. (6)):

$$TS = S1 + S2 \tag{6}$$

The relative contents of TOC, S1, S2, and TS (represented by TOC-P, S1-P, S2-P, and TS-P, respectively) of SOM, MOM and POM represent the relative abundances and hydrocarbon contributions of OM with the three occurrence types. The calculation equations are shown below (Eq. (7)–Eq.(10)):

$$(TOC\text{-}P_{SOM}, TOC\text{-}P_{MOM}, TOC\text{-}P_{POM}) = (TOC_{SOM}, TOC_{MOM}, TOC_{POM}) / TOC_r \cdot 100\% \tag{7}$$
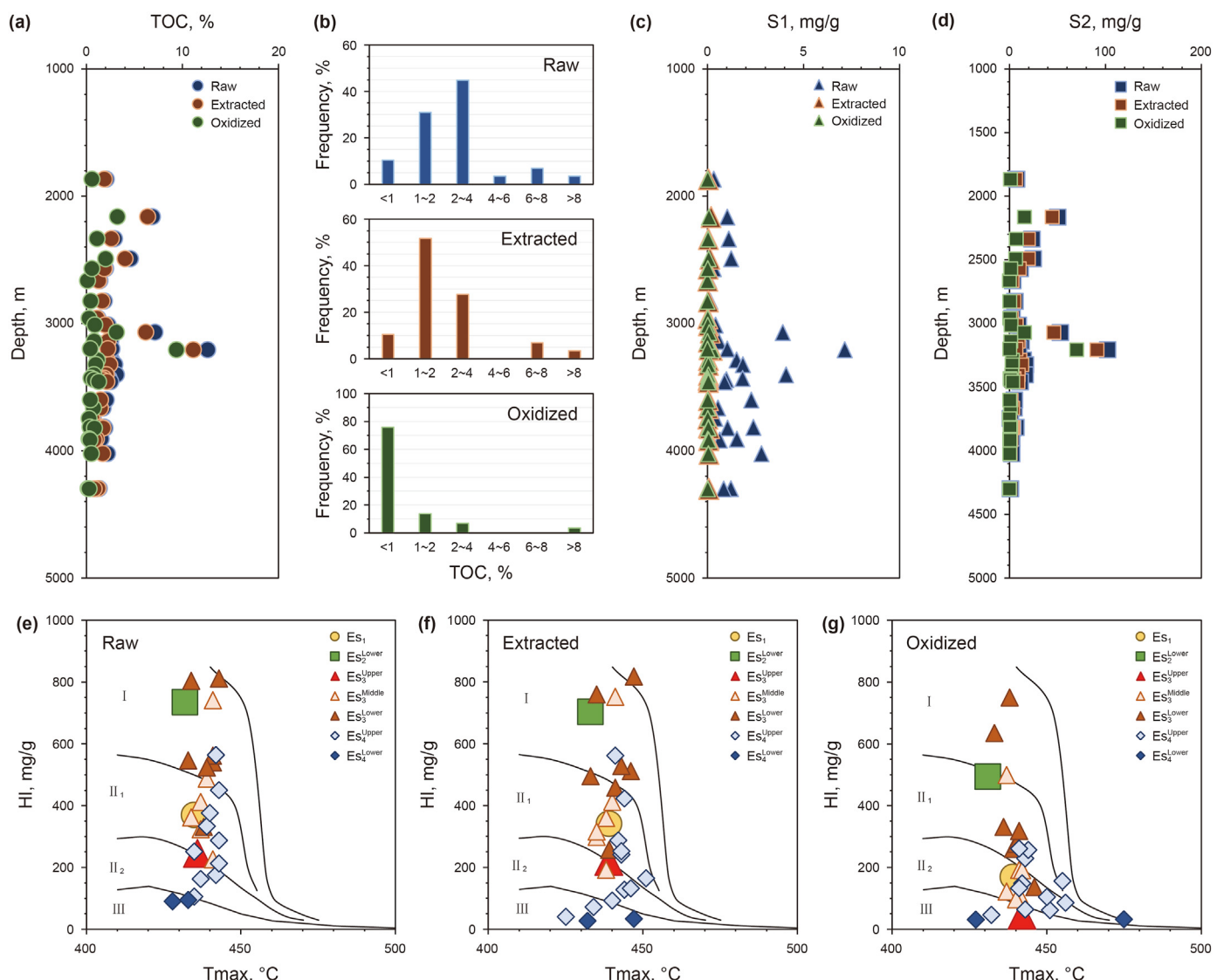
Fig. 2. OM and hydrocarbon characteristics of the raw samples (Raw), Soxhlet extracted samples (Extracted) and Na$_2$S$_2$O$_8$ oxidized samples (Oxidized): (**a**) variation of TOC with increasing depth, (**b**) frequency distribution of TOC, (**c**) variation of S1 with increasing depth, (**d**) variation of S2 with increasing depth, and (**e**, **f**, **g**) kerogen types determined by HI vs T$_{max}$ in the raw, extracted and oxidized samples. The data are given in Table S1 in the Supplementary Data.

$$(S1\text{-}P_{SOM}, S1\text{-}P_{MOM}, S1\text{-}P_{POM}) = (S1_{SOM}, S1_{MOM}, S1_{POM}) / S1_r \cdot 100\% \ (8)$$

$$(S2\text{-}P_{SOM}, S2\text{-}P_{MOM}, S2\text{-}P_{POM}) = (S2_{SOM}, S2_{MOM}, S2_{POM}) / S2_r \cdot 100\% \ (9)$$

$$(TS\text{-}P_{SOM}, TS\text{-}P_{MOM}, TS\text{-}P_{POM}) = (TS_{SOM}, TS_{MOM}, TS_{POM}) / TS_r \cdot 100\% (10)$$

The quantification results are shown in Table S2 in the Supplementary Data.

4.3. Comparison of the abundances and hydrocarbon contributions of SOM, MOM, and POM

4.3.1. Relative abundances of SOM, MOM, and POM
The relative abundances of SOM, MOM, and POM are approximately 17.62%, 54.41%, and 27.97% on average, respectively, revealing that MOM accounts for the largest OM abundance in the source rocks (Fig. 5a).

For samples with different kerogen types, the relative content of each occurrence type of OM would also be different. For example, in samples with type I kerogen, most of the SOM content is in the range of 0–25%, and the POM and MOM contents are in the 25%–40% and 40%–75% ranges, respectively (Fig. 5d). In samples with type II$_1$ and II$_2$ kerogen, the SOM content is mainly in the range of 0–25%, the POM content is in the 0–50% range and the MOM content is in the 35%–85% (Fig. 5d). In samples with type III kerogen, it is evident that the MOM content is the largest, with a range of 50%–80% (Fig. 5d). The average abundance of different occurrences of OM shows that $TOC\text{-}P_{MOM} > TOC\text{-}P_{POM} > TOC\text{-}P_{SOM}$ in samples with kerogen I and II, and $TOC\text{-}P_{MOM} > TOC\text{-}P_{SOM} > TOC\text{-}P_{POM}$ in samples with kerogen III (Fig. 5b). These characteristics indicate that MOM contributes the largest amount of OM, regardless of the type of kerogen in mudstones.

In addition, the relative abundances of SOM, MOM, and POM are also different in different layers. The SOM contents in the four sub-members of Es are mainly in the range of 0–25% (Fig. 5e). In Es$_3^{Middle}$, the MOM content is 50%–75%, and the POM content is 10%–35%; in Es$_3^{Lower}$, the MOM content is mainly 25%–55%, and the POM content is 25%–65%; in Es$_4^{upper}$, some of the MOM content is in
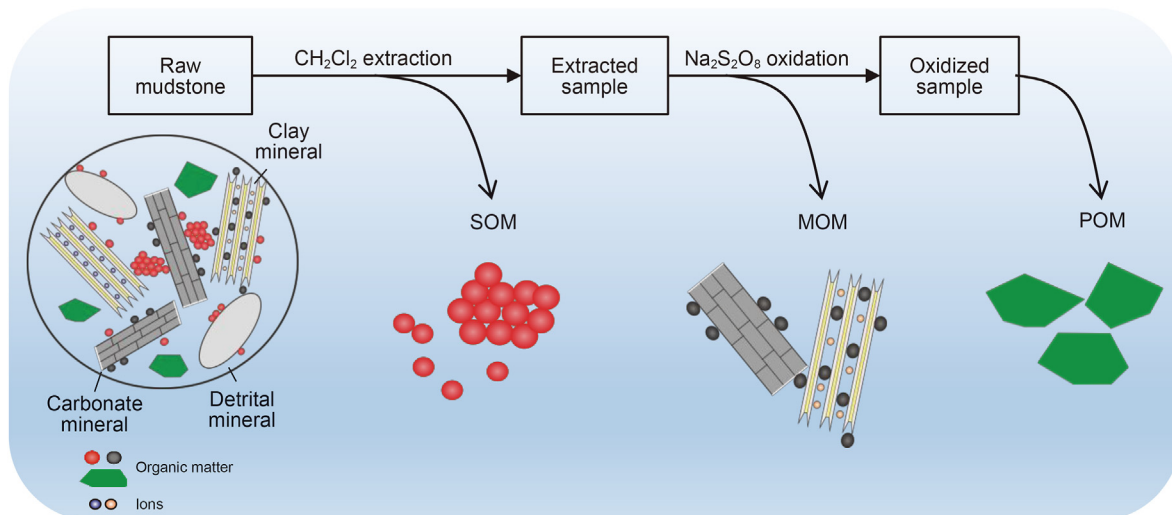
Fig. 3. Schematic of OM with different occurrences in mudstones (modified from Cai et al. (2020), Keil and Mayer (2014), and Zhu et al. (2016)).
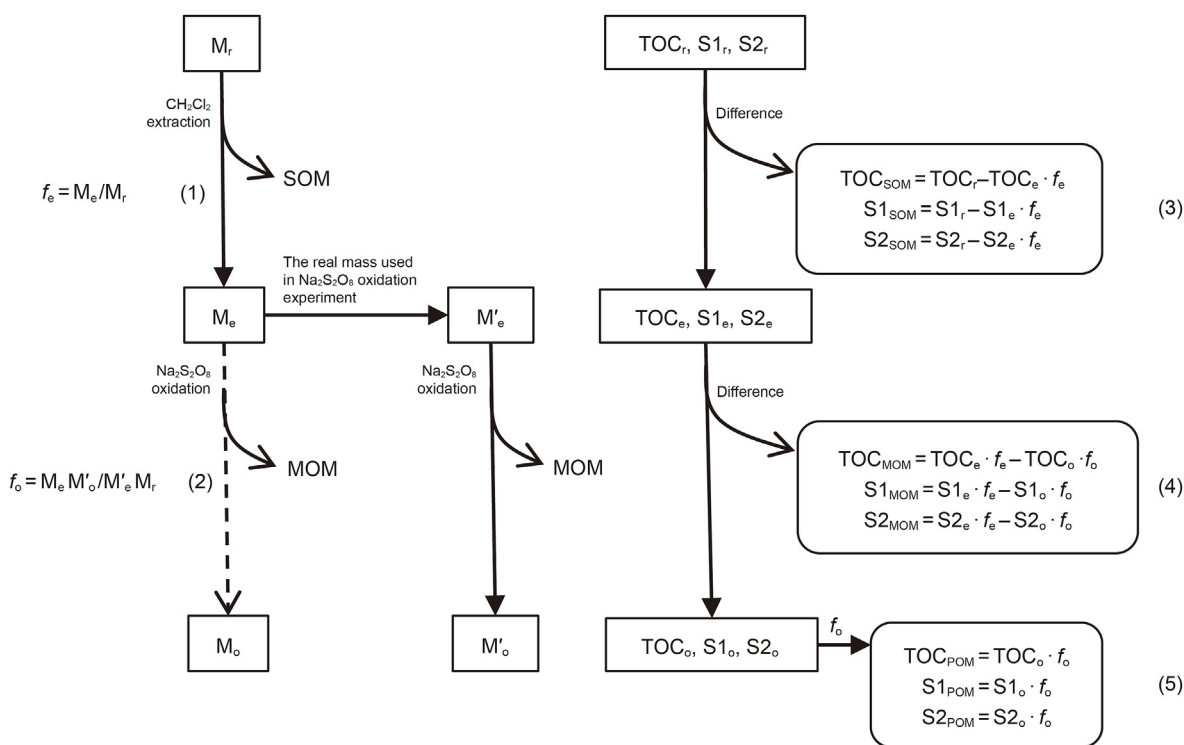

Fig. 4. Calculation process of the abundance and hydrocarbon content of SOM, MOM, and POM (M_r, M_e: mass of the raw and extracted samples in the Soxhlet extraction experiment; M_e', M_o': mass of the extracted and oxidized samples in the $Na_2S_2O_8$ oxidation experiment; M_o: mass of the oxidized samples if all the extracted samples (mass of M_e) were used in the $Na_2S_2O_8$ oxidation experiment; (TOC_r, $S1_r$, and $S2_r$), (TOC_e, $S1_e$, and $S2_e$), (TOC_o, $S1_o$, and $S2_o$): TOC, S1, and S2 of the raw, extracted, and oxidized samples, respectively; (TOC_{SOM}, $S1_{SOM}$, and $S2_{SOM}$), (TOC_{MOM}, $S1_{MOM}$, and $S2_{MOM}$), (TOC_{POM}, $S1_{POM}$, and $S2_{POM}$): abundance, free hydrocarbons and pyrolysis hydrocarbons of SOM, MOM, and POM, respectively; f_e, f_o: conversion factor of TOC, S1, and S2 of the extracted and oxidized samples).

the range of 50%–75% and the POM content is less than 25%, and some of the MOM content is in the range of 40%–50% and the POM content is in the range of 25%–50%; in Es_4^{Lower}, the MOM content is in the range of 50%–80%, and the POM and SOM contents are in the range of 0–25% (Fig. 5e). The average contents of SOM, MOM, and POM are $TOC\text{-}P_{MOM} > TOC\text{-}P_{POM} > TOC\text{-}P_{SOM}$ in Es_3^{Middle}, Es_3^{Lower} and Es_4^{upper} and $TOC\text{-}P_{MOM} > TOC\text{-}P_{SOM} > TOC\text{-}P_{POM}$ in Es_4^{Lower} (Fig. 5c). The results suggest that although the distribution ranges of SOM,

MOM, and POM contents are different in the four layers, MOM also accounts for the majority of the OM in each layer.

4.3.2. Relative hydrocarbon contents produced by SOM, MOM, and POM

The hydrocarbon quantification results show that the average $S1\text{-}P$ of SOM is approximately 92.28%, which is much larger than the $S1\text{-}P$ of MOM and POM, which are 5.01% and 2.71%, respectively
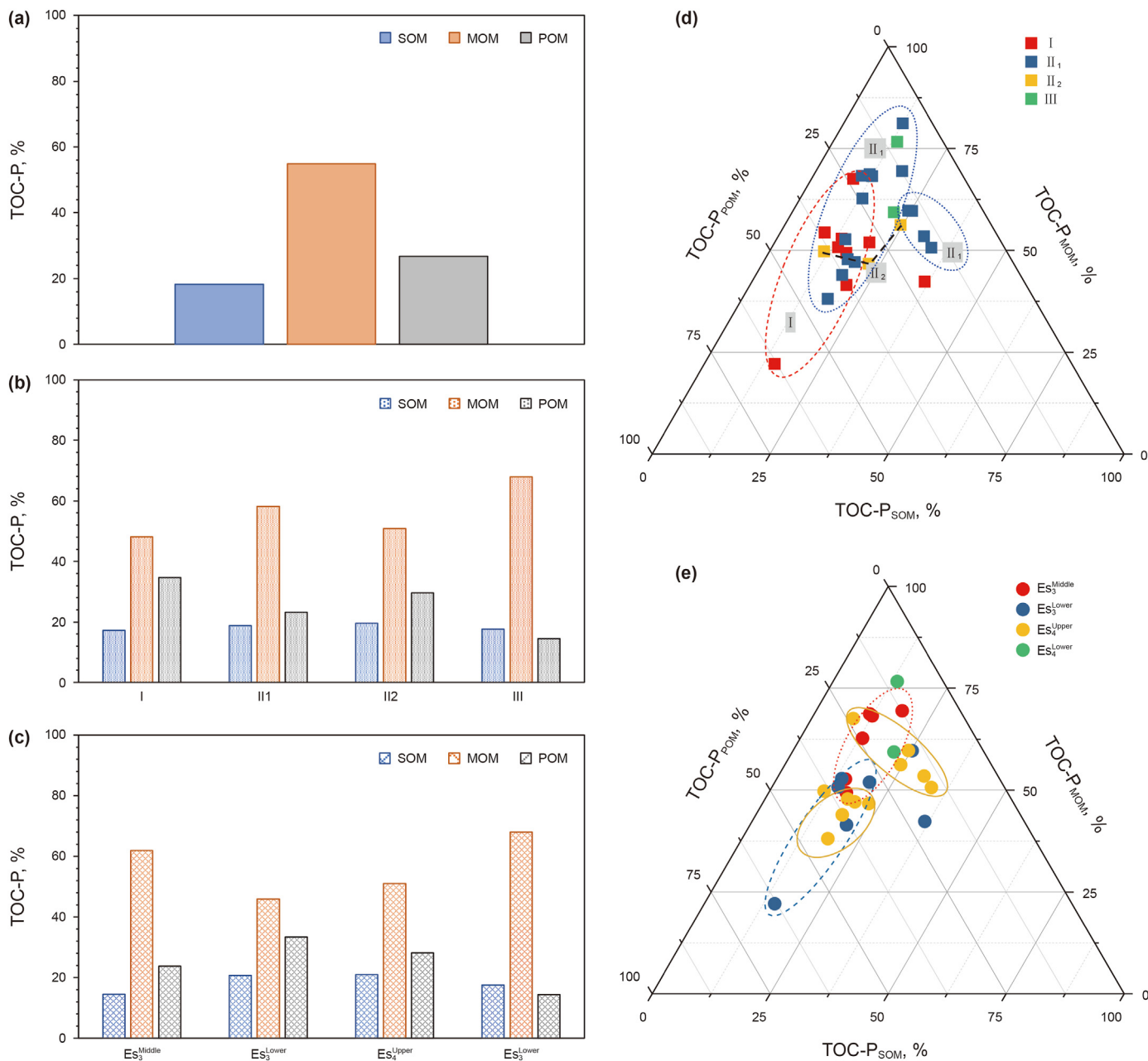
Fig. 5. Characteristics of the abundance of SOM, MOM, and POM in mudstones: (**a**) average contents of SOM, MOM, and POM in mudstone samples; (**b, c**) average content of SOM, MOM, and POM in mudstones with different types of kerogen and different layers; (**d, e**) abundance distribution of SOM, MOM, and POM in mudstones with different types of kerogen and different layers.

(Fig. 6a). SOM contributes more than 90% S1 on average to samples with each type of kerogen (Fig. 6b) and contributes more than 87% S1 to samples in each layer (Fig. 6c). This reveals that SOM is the main contributor of S1, regardless of the type of kerogen or layer of the mudstones.

The total $S2\text{-}P$ data illustrate that 34.72% S2 is from SOM, 50.38% is from MOM and 14.90% is from POM on average, which indicates that MOM generates more S2 than SOM and POM averagely (Fig. 6a). With the kerogen type changing from I to II_1, II_2 and III in an orderly manner, the contribution of SOM to the S2 increases, while the contribution of MOM and POM to the S2 decreases (Fig. 6d). In addition, with the layers changing from Es_3^{Middle}, Es_3^{Lower}, and Es_4^{upper} to Es_4^{Lower}, the S2 generated from SOM increases, while the S2 generated from MOM decreases (Fig. 6e). The

contribution of POM to S2 increases from Es_3^{Middle} to Es_3^{Lower} and then decreases in Es_4^{upper} and Es_4^{Lower} (Fig. 6e).

TS reveals the characteristics of the total hydrocarbons generated from SOM, MOM and POM. The average $TS\text{-}P$ content shows that SOM, MOM and POM contribute 40.56%, 45.91% and 13.53% hydrocarbons, respectively (Fig. 6a). The contributions of SOM and MOM to total hydrocarbon generation are similar and much larger than that of POM. With the kerogen type changing from I to II_1, II_2 and III, the TS contribution of SOM increases, and the TS contents of MOM and POM decrease (Fig. 6f). In addition, in samples with type I and II_1 kerogen, MOM contributes more TS than SOM, but the opposite is true in samples with type II_2 and III kerogen (Fig. 6f). With the layers changing from Es_3^{Middle}, Es_3^{Lower}, and Es_4^{upper} to Es_4^{Lower}, the TS contribution of SOM increases, and the contribution
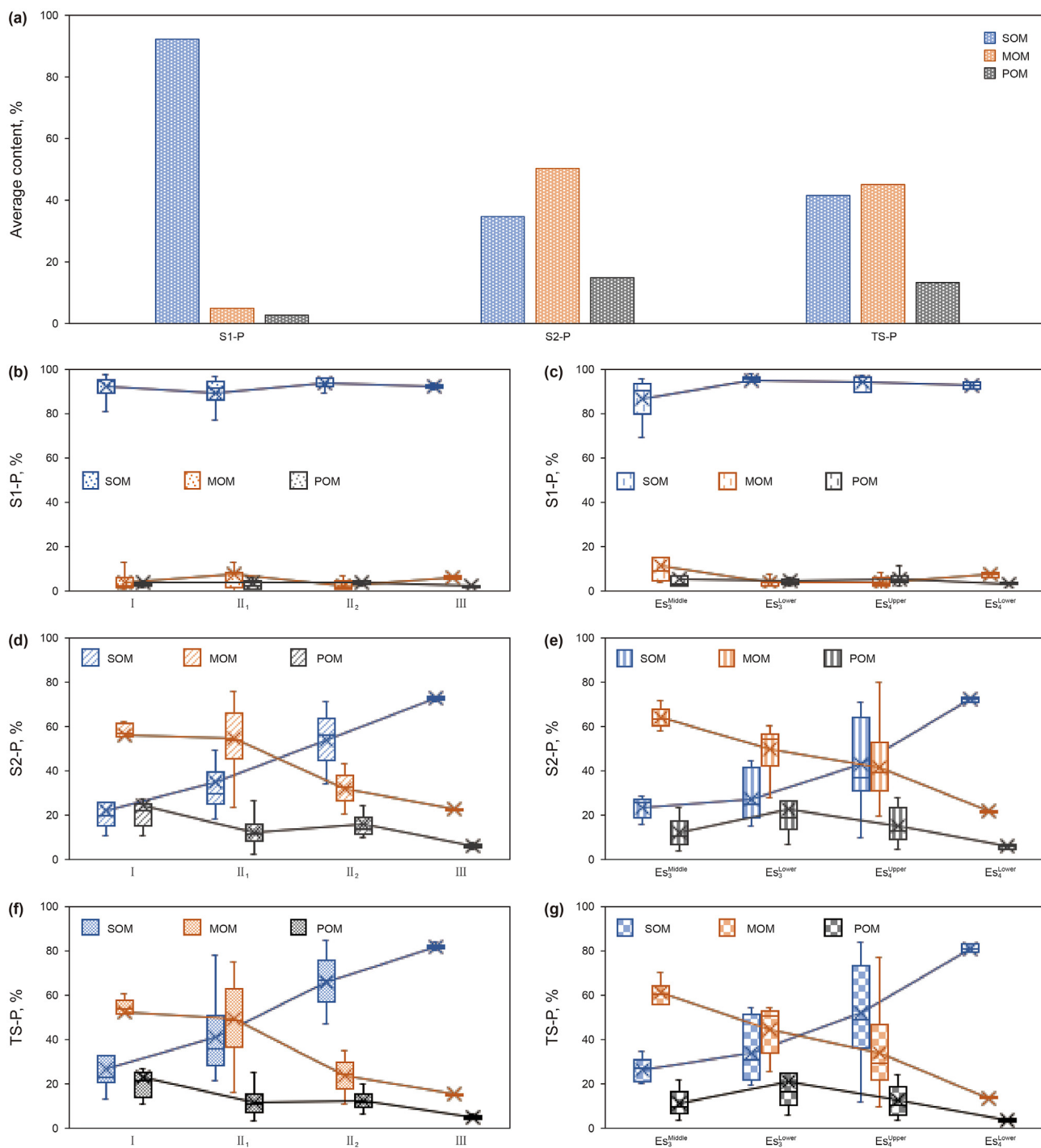
Fig. 6. Characteristics of the relative hydrocarbon contents generated by SOM, MOM, and POM. (**a**) Average contents of $S1$-P, $S2$-P, and TS-P of the total mudstone samples; (**b, d, f**) distribution and average contents of $S1$-P, $S2$-P, and TS-P in mudstones with different types of kerogens; (**c, e, g**) distribution and average contents of $S1$-P, $S2$-P, and TS-P in mudstones of different layers.

of MOM and POM decrease (Fig. 6g). POM contributes the least to TS among the three occurrence types of OM in mudstones with different kerogen types and different layers (Fig. 6f and g).

The abundances and hydrocarbon characteristics of different occurrence types of OM reveal that SOM and MOM are the main contributors to hydrocarbon generation, S1 is mainly generated from SOM and S2 is mostly generated from MOM. Although the relative abundance of POM is mostly larger than that of SOM, POM still produces the fewest hydrocarbons. Moreover, the total hydrocarbon content of SOM and MOM alternately changes in

mudstones with different kerogen types and different layers. In general, the hydrocarbon contributions of OM with the three occurrences in mudstones have great differences.

4.4. Evolutionary differences of the hydrocarbons generated from SOM, MOM, and POM

In the whole depth profile, S1 is mostly generated from SOM, while little is generated from MOM and POM (Fig. 7a, b, c), which is consistent with the trend of the average $S1$-P content of OM with
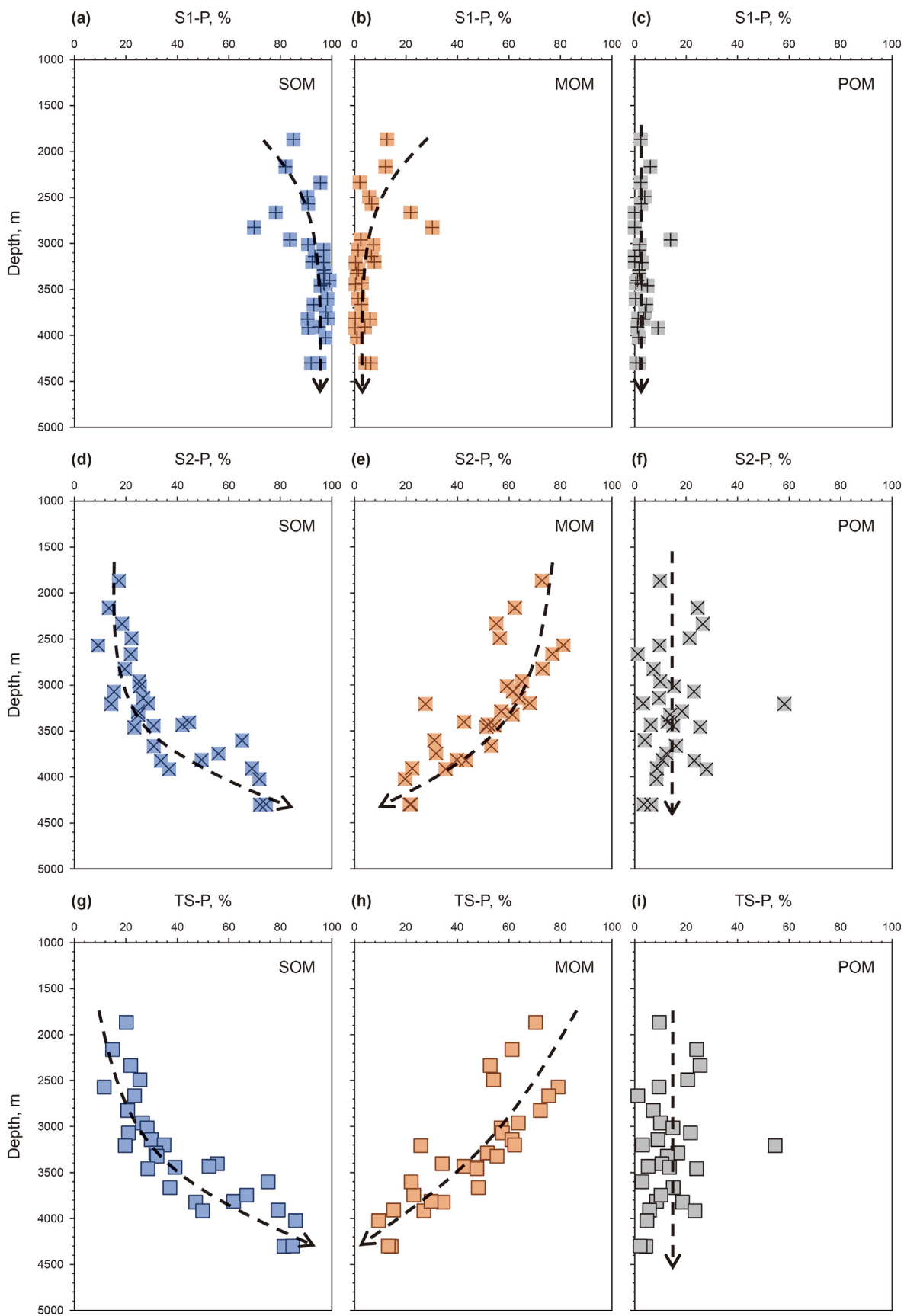
Fig. 7. Evolution of S1, S2, and TS of (**a**, **d**, **g**) SOM, (**b**, **e**, **h**) MOM, and (**c**, **f**, **i**) POM.
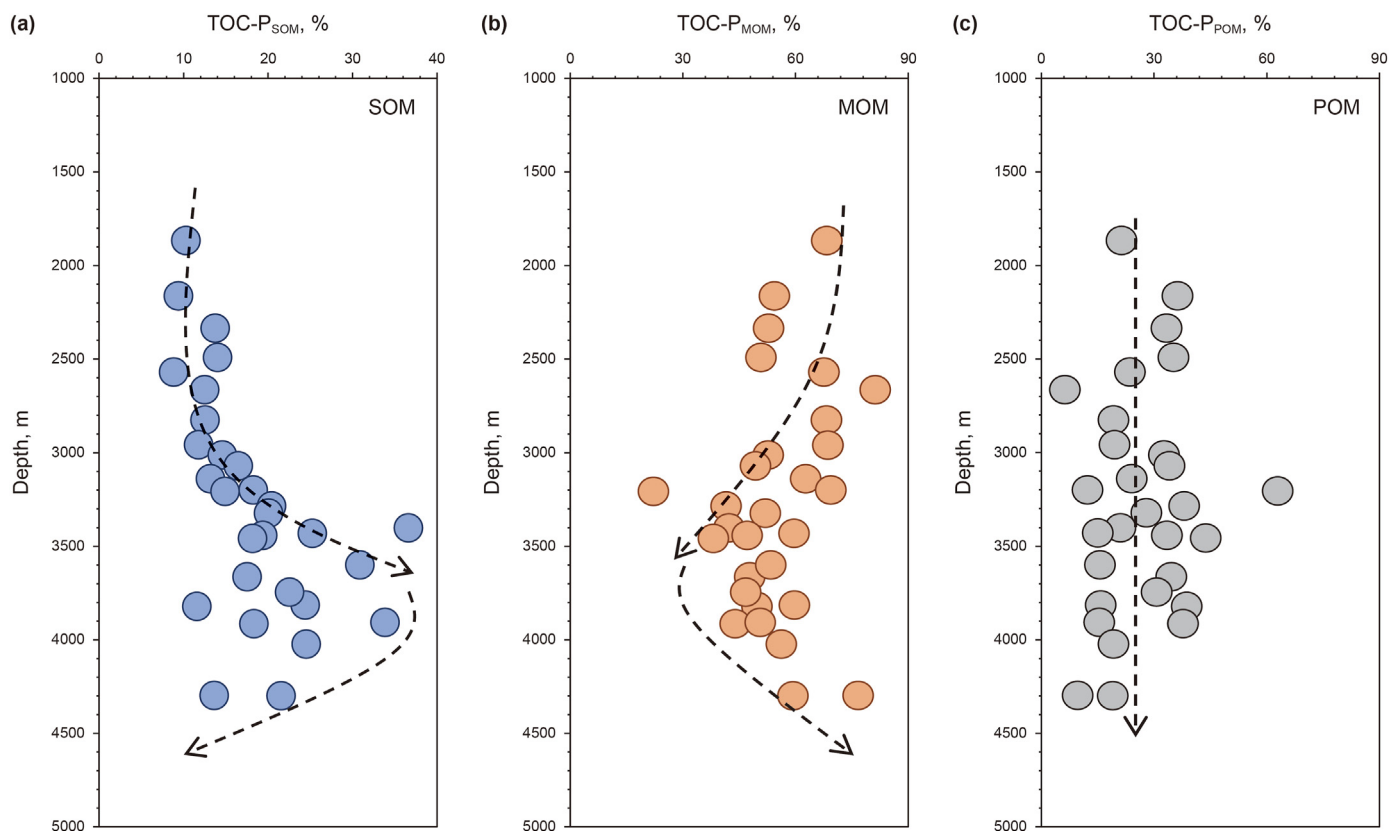
Fig. 8. Evolution of the relative abundance of (**a**) SOM, (**b**) MOM, and (**c**) POM.
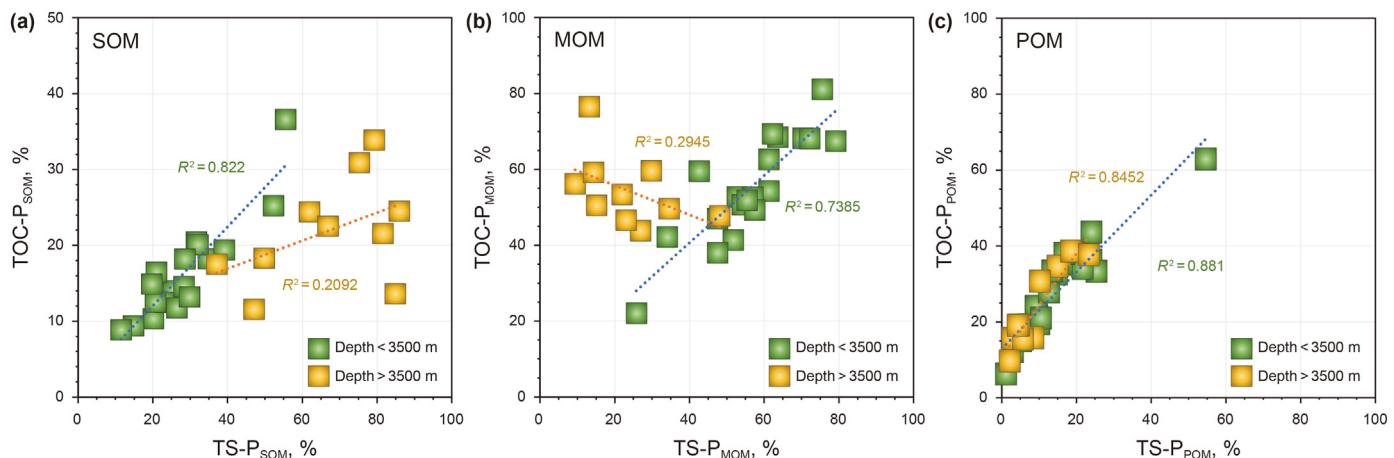

Fig. 9. Correlations of the relative abundance of OM and the relative hydrocarbon contents of OM with the three occurrence types: (**a**) SOM, (**b**) MOM, and (**c**) POM.

the three occurrence types mentioned above. $S2\text{-}P$ of SOM increases and $S2\text{-}P$ of MOM decreases with depth (Fig. 7d and e). $S2\text{-}P$ of most POM is less than 30% and has no evident change throughout the whole depth (Fig. 7f). In addition, at depths less than 3500 m, the S2 content contributed by SOM is less than 30%, and MOM contributes more than 50% of S2. At depths deeper than 3500 m, SOM-contributed S2 increases, even to 80%, and MOM-contributed S2 decreases to 20%. These characteristics suggest that MOM plays the main role in S2 generation at shallow depths, and SOM makes the greatest contribution to S2 generation at deep depths. The evolutionary trend of $TS\text{-}P$ is completely similar to that of $S2\text{-}P$ (Fig. 7g, h,

i), which implies that MOM and SOM would be the main precursors of the total hydrocarbons in shallow and deep depths, respectively, and that POM contributes fewer hydrocarbons at the whole depth.

The abundance of each occurrence type of OM would be an important factor affecting the differences in hydrocarbon evolution. At depths less than 3500 m, the relative content of SOM increases and MOM decreases, which coincides with the evolution of SOM-contributed and MOM-contributed hydrocarbons (Fig. 7g and h and Fig. 8a and b). $TOC\text{-}P$ and $TS\text{-}P$ also show a positive correlation for SOM and MOM, respectively (Fig. 9a and b). At depths deeper than 3500 m, the relative content of SOM decreases and MOM

increases, which evolves oppositely to the *TS-P* of SOM and MOM (Fig. 7g and h and Fig. 8a and b), and the correlation of *TOC-P* and *TS-P* is poor for SOM and MOM (Fig. 9a and b). This reveals that the abundance of SOM and MOM would be an important factor influencing the hydrocarbon content at shallow depths, while there must be other important factors that mainly influence the hydrocarbon content contributed by SOM and MOM in deep depths. As the *TOC-P* and *TS-P* of POM have the same evolutionary trend (Figs. 7i and 8c) and the two parameters have high correlations in both shallow and deep depths (Fig. 9c), the abundance of POM would also be an important factor in its hydrocarbon content.

The hydrocarbon characteristics of OM with the three occurrence types indicate that kerogen types and different layers influence the hydrocarbon contributions of SOM, MOM, and POM, which demonstrates that the depositional environment of the layer and the burial evolution may also influence the hydrocarbon evolution of SOM, MOM, and POM. In addition, previous studies have revealed that a large amount of OM is adsorbed in the interlayer space of smectite (Cai et al., 2007; Keil and Mayer, 2014; Kennedy et al., 2002). During burial evolution, smectite converts to illite and simultaneously releases interlayer OM (Yariv and Cross, 2002). The solid acid in smectite could also catalyze the interlayer OM to generate hydrocarbons (Bu et al., 2017; Du et al., 2021). The smectite illitization process appears largely in Es_3^{Middle} and Es_3^{Lower} in the Dongying Sag, and is also in the depth range of 2000–3400 m (Li et al., 2017). The evolution of clay minerals significantly influences on the hydrocarbon generation of MOM at shallow depths. In deep depths, the environment of the Dongying Sag becomes closed, overpressure, and high temperature (Guo et al., 2010). SOM could have produced more hydrocarbons under such conditions, and MOM would have also gradually transformed to SOM (Zhu et al., 2020). All these environmental and evolutionary factors make SOM the main precursor of hydrocarbon generation at deep depths. In short, OM with the three occurrence types evolve out of sync in different burial processes, leading to the different hydrocarbon evolutions of SOM, MOM, and POM.

5. Conclusions

This work quantified OM with the three types of occurrences, namely, SOM, MOM, and POM, in mudstones by using Soxhlet extraction and $Na_2S_2O_8$ oxidation sequentially and conducting Rock-Eval VI pyrolysis on the raw, extracted, and oxidized samples, respectively.

In mudstones with different types of kerogen and mudstones in different layers, the abundance of MOM is the largest. The hydrocarbon contributions of SOM, MOM, and POM are quite different. SOM contributes most of the S1, and MOM generates the most S2. SOM and MOM contribute most of the TS, and POM contributes little to TS. This reveals that SOM and MOM are the main hydrocarbon precursors. Additionally, the hydrocarbon contributions of SOM and MOM change alternately as the kerogen types change from I, II$_1$, and II$_2$ to III, and as the layers change from Es_3^{Middle}, Es_3^{Lower}, and Es_4^{upper} to Es_4^{Lower}.

MOM-contributed hydrocarbons are numerous at shallow depths and decrease to nearly zero at greater depths; the trend for SOM-contributed hydrocarbons is in the other direction, with these hydrocarbons occurring at great depths; POM-contributed hydrocarbons show little change throughout the entire depth range. This demonstrates that MOM should be the main hydrocarbon precursor in shallow formations and that SOM is the main hydrocarbon contributor at deep depths. Moreover, the abundance of each occurrence type of OM is related to the local stratigraphy, and burial evolution plays a considerable role in the transformation of each hydrocarbon precursor.

Appendix A. Supplementary data

Supplementary Data to this article can be found online at https://doi.org/10.1016/j.petsci.2022.02.006.

References

Arnarson, T.S., Keil, R.G., 2001. Organic–mineral interactions in marine sediments studied using density fractionation and X-ray photoelectron spectroscopy. Org. Geochem. 32, 1401–1415. https://doi.org/10.1016/S0146-6380(01)00114-0.

Bai, C.Y., Yu, B.S., Liu, H.M., et al., 2018. The genesis and evolution of carbonate minerals in shale oil formations from Dongying depression, Bohai Bay Basin, China. Int. J. Coal Geol. 189, 8–26. https://doi.org/10.1016/j.coal.2018.02.008.

Behar, F., Beaumont, V., Penteado, H.L.B., 2001. Rock-Eval 6 technology: performances and developments. Oil Gas Sci. Technol.-Rev. IFP 56, 111–134. https://doi.org/10.2516/ogst:2001013.

Berthonneau, J., Grauby, O., Abuhaikal, M., et al., 2016. Evolution of organo-clay composites with respect to thermal maturity in type II organic-rich source rocks. Geochem. Cosmochim. Acta 195, 68–83. https://doi.org/10.1016/j.gca.2016.09.008.

Bu, H.L., Yuan, P., Liu, H.M., et al., 2017. Effects of complexation between organic matter (OM) and clay mineral on OM pyrolysis. Geochem. Cosmochim. Acta 212, 1–15. https://doi.org/10.1016/j.gca.2017.04.045.

Cai, J.G., Bao, Y.J., Yang, S.Y., et al., 2007. Research on preservation and enrichment mechanisms of organic matter in muddy sediment and mudstone. Sci. China Earth Sci. 50, 765–775. https://doi.org/10.1007/s11430-007-0005-0.

Cai, J.G., Chao, Q., Wang, Y.S., et al., 2021. Method for Separating and Quantifying Organic Matters in Different Occurrence States in Hydrocarbon Source Rock, vol. 6. Patent No, China, 1488506.

Cai, J.G., Zhu, X.J., Zhang, J.Q., et al., 2020. Heterogeneities of organic matter and its occurrence forms in mudrocks: evidence from comparisons of palynofacies. Mar. Petrol. Geol. 111, 21–32. https://doi.org/10.1016/j.marpetgeo.2019.08.004.

Cambardella, C.A., Elliott, E.T., 1992. Particulate soil organic-matter changes across a grassland cultivation sequence. Soil Sci. Soc. Am. J. 56, 777–783. https://doi.org/10.2136/sssaj1992.03615995005600030017x.

Carrie, J., Sanei, H., Stern, G., 2012. Standardisation of Rock–Eval pyrolysis for the analysis of recent sediments and soils. Org. Geochem. 46, 38–53. https://doi.org/10.1016/j.orggeochem.2012.01.011.

Carter, M.R., Angers, D.A., Gregorich, E.G., et al., 2003. Characterizing organic matter retention for surface soils in eastern Canada using density and particle size fractions. Can. J. Soil Sci. 83, 11–23. https://doi.org/10.4141/S01-087.

Du, J.Z., Cai, J.G., Lei, T.Z., et al., 2021. Diversified roles of mineral transformation in controlling hydrocarbon generation process, mechanism, and pattern. Geosci. Front. 12, 725–736. https://doi.org/10.1016/j.gsf.2020.08.009.

Du, P.Y., Cai, J.G., Liu, Q., et al., 2019. The role transformation of soluble organic matter in the process of hydrocarbon generation in mud source rock. Petrol. Sci. Technol. 37, 1800–1807. https://doi.org/10.1080/10916466.2019.1602637.

Durand, B., 1980. Kerogen: Insoluble Organic Matter from Sedimentary Rocks. Editions technip, France.

Eusterhues, K., Rumpel, C., Kleber, M., et al., 2003. Stabilisation of soil organic matter by interactions with minerals as revealed by mineral dissolution and oxidative degradation. Org. Geochem. 34, 1591–1600. https://doi.org/10.1016/j.orggeochem.2003.08.007.

Feng, Y.L., Li, S.T., Lu, Y.C., 2013. Sequence stratigraphy and architectural variability in late eocene lacustrine strata of the dongying depression, Bohai Bay Basin, Eastern China. Sediment. Geol. 295, 1–26. https://doi.org/10.1016/j.sedgeo.2013.07.004.

Guo, X.W., He, S., Liu, K.Y., et al., 2010. Oil generation as the dominant overpressure mechanism in the cenozoic dongying depression, Bohai Bay Basin, China. AAPG Bull. 94, 1859–1881. https://doi.org/10.1306/05191009179.

Helfrich, M., Flessa, H., Mikutta, R., et al., 2007. Comparison of chemical fractionation methods for isolating stable soil organic carbon pools. Eur. J. Soil Sci. 58, 1316–1329. https://doi.org/10.1111/j.1365-2389.2007.00926.x.

Jarvie, D.M., Hill, R.J., Ruble, T.E., et al., 2007. Unconventional shale-gas systems: the Mississippian Barnett Shale of north-central Texas as one model for thermogenic shale-gas assessment. AAPG Bull. 91, 475–499. https://doi.org/10.1306/12190606068.

Kaiser, K., Mikutta, R., Guggenberger, G., 2007. Increased stability of organic matter sorbed to ferrihydrite and goethite on aging. Soil Sci. Soc. Am. J. 71, 711–719. https://doi.org/10.2136/sssaj2006.0189.

Keil, R.G., Mayer, L.M., 2014. 12.12 - mineral matrices and organic matter. In: Holland, H.D., Turekian, K.K. (Eds.), Treatise on Geochemistry, second ed. Elsevier, Oxford, pp. 337–359. https://doi.org/10.1016/B978-0-08-095975-

7.01024-X.

Kennedy, M.J., Löhr, S.C., Fraser, S.A., et al., 2014. Direct evidence for organic carbon preservation as clay-organic nanocomposites in a Devonian black shale; from deposition to diagenesis. Earth Planet Sci. Lett. 388, 59–70. https://doi.org/10.1016/j.epsl.2013.11.044.

Kennedy, M.J., Pevear, D.R., Hill, R.J., 2002. Mineral surface control of organic carbon in black shale. Science 295, 657. https://doi.org/10.1126/science.1066611.

Kennedy, M.J., Wagner, T., 2011. Clay mineral continental amplifier for marine carbon sequestration in a greenhouse ocean. Proc. Natl. Acad. Sci. U. S. A. 108, 9776. https://doi.org/10.1073/pnas.1018670108.

Kiem, R., Knicker, H., Kögel-Knabner, I., 2002. Refractory organic carbon in particle-size fractions of arable soils I: distribution of refractory carbon between the size fractions. Org. Geochem. 33, 1683–1697. https://doi.org/10.1016/S0146-6380(02)00113-4.

Kleber, M., Sollins, P., Sutton, R., 2007. A conceptual model of organo-mineral interactions in soils: self-assembly of organic molecular fragments into zonal structures on mineral surfaces. Biogeochemistry. 85, 9–24. https://doi.org/10.1007/s10533-007-9103-5.

Li, Y.L., Cai, J.G., Song, G.Q., et al., 2015. DRIFT spectroscopic study of diagenetic organic-clay interactions in argillaceous source rocks. Spectroc Acta Pt A-Molec Biomolec Spectr 148, 138–145. https://doi.org/10.1016/j.saa.2015.03.131.

Li, Y.L., Cai, J.G., Wang, X.J., et al., 2017. Smectite-illitization difference of source rocks developed in saline and fresh water environments and its influence on hydrocarbon generation: a study from the Shahejie Formation, Dongying Depression, China. Mar. Petrol. Geol. 80, 349–357. https://doi.org/10.1016/j.marpetgeo.2016.12.004.

Lopez-Sangil, L., Rovira, P., 2013. Sequential chemical extractions of the mineral-associated soil organic matter: an integrated approach for the fractionation of organo-mineral complexes. Soil Biol. Biochem. 62, 57–67. https://doi.org/10.1016/j.soilbio.2013.03.004.

Lützow, M.V., Kögel-Knabner, I., Ekschmitt, K., et al., 2007. SOM fractionation methods: relevance to functional pools and to stabilization mechanisms. Soil Biol. Biochem. 39, 2183–2207. https://doi.org/10.1016/j.soilbio.2007.03.007.

Lützow, M.V., Kögel-Knabner, I., Ekschmitt, K., et al., 2006. Stabilization of organic matter in temperate soils: mechanisms and their relevance under different soil conditions-a review. Eur. J. Soil Sci. 57, 426–445. https://doi.org/10.1111/j.1365-2389.2006.00809.x.

Meier, L.P., Menegatti, A.P., 1997. A new, efficient, one-step method for the removal of organic matter from clay-containing sediments. Clay Miner. 32, 557–563. https://doi.org/10.1180/claymin.1997.032.4.06.

Menegatti, A.P., Frueh-Green, G.L., Stille, P., 1999. Removal of organic matter by disodium peroxodisulphate; effects on mineral structure, chemical composition and physicochemical properties of some clay minerals. Clay Miner. 34, 247–257. https://doi.org/10.1180/000985599546217.

Mikutta, R., Kleber, M., Kaiser, K., et al., 2005. Review: organic matter removal from soils using hydrogen peroxide, sodium hypochlorite, and disodium peroxodisulfate. Soil Sci. Soc. Am. J. 69, 120–135. https://doi.org/10.2136/sssaj2005.0120.

Mikutta, R., Mikutta, C., Kalbitz, K., et al., 2007. Biodegradation of forest floor organic matter bound to minerals via different binding mechanisms. Geochem. Cosmochim. Acta. 71, 2569–2590. https://doi.org/10.1016/j.gca.2007.03.002.

Mikutta, R., Schaumann, G.E., Gildemeister, D., et al., 2009. Biogeochemistry of mineral–organic associations across a long-term mineralogical soil gradient (0.3–4100kyr), Hawaiian Islands. Geochem. Cosmochim. Acta. 73, 2034–2060. https://doi.org/10.1016/j.gca.2008.12.028.

Rahman, H.M., Kennedy, M.J., Löhr, S.C., et al., 2017. Clay-organic association as a control on hydrocarbon generation in shale. Org. Geochem. 105, 42–55. https://doi.org/10.1016/j.orggeochem.2017.01.011.

Rahman, H.M., Kennedy, M.J., Löhr, S.C., et al., 2018. The influence of shale depositional fabric on the kinetics of hydrocarbon generation through control of mineral surface contact area on clay catalysis. Geochem. Cosmochim. Acta. 220, 429–448. https://doi.org/10.1016/j.gca.2017.10.012.

Sebag, D., Copard, Y., Di-Giovanni, C., et al., 2006. Palynofacies as useful tool to study origins and transfers of particulate organic matter in recent terrestrial environments: synopsis and prospects. Earth Sci. Rev. 79, 241–259. https://doi.org/10.1016/j.earscirev.2006.07.005.

Tissot, B.P., Welte, D.H., 1984. Petroleum Formation and Occurrence. Sprioger-Verlag, Berlin.

Tyson, R.V., 1995. Sedimentary organic matter: organic facies and palynofacies. Springer Science & Business Media.

Yariv, S., Cross, H., 2001. Organo-clay Complexes and Interactions. CRC Press.

Yuan, P., Liu, H.M., Liu, D., et al., 2013. Role of the interlayer space of montmorillonite in hydrocarbon generation: an experimental study based on high temperature–pressure pyrolysis. Appl. Clay Sci. 75–76, 82–91. https://doi.org/10.1016/j.clay.2013.03.007.

Zeng, X., Cai, J.G., Dong, Z., et al., 2018. Relationship between mineral and organic matter in shales: the case of Shahejie Formation, dongying sag, China. Minerals. 8, 222. https://doi.org/10.3390/min8060222.

Zhang, L.Y., Liu, Q., Zhu, R.F., et al., 2009. Source rocks in mesozoic–cenozoic continental rift basins, east China: a case from dongying depression, Bohai Bay Basin. Org. Geochem. 40, 229–242. https://doi.org/10.1016/j.orggeochem.2008.10.013.

Zhu, X.J., Cai, J.G., Liu, W.X., et al., 2016. Occurrence of stable and mobile organic matter in the clay-sized fraction of shale: significance for petroleum geology and carbon cycle. Int. J. Coal Geol. 160, 1–10. https://doi.org/10.1016/j.coal.2016.03.011.

Zhu, X.J., Cai, J.G., Wang, Y.S., et al., 2020. Evolution of organic-mineral interactions and implications for organic carbon occurrence and transformation in shale. Geol. Soc. Am. Bull. 132, 784–792. https://doi.org/10.1130/B35223.1.

Zou, Y.R., Sun, J.N., Li, Z., et al., 2018. Evaluating shale oil in the Dongying Depression, Bohai Bay Basin, China, using the oversaturation zone method. J. Petrol. Sci. Eng. 161, 291–301. https://doi.org/10.1016/j.petrol.2017.11.059.